In Depth Analysis of Food Structures
Hyperspectral Subsurface Laser Scattering

Otto Højager Attermann Nielsen[1], Anders Lindbjerg Dahl[1], Rasmus Larsen[1], Flemming Møller[2], Frederik Donbæk Nielsen[3], Carsten L. Thomsen[3], Henrik Aanæs[1] and Jens Michael Carstensen[1]

[1]DTU Informatics, Technical University of Denmark
[2] DANISCO A/S, [3] NKT Photonics A/S

Abstract. In this paper we describe a computer vision system based on SLS (Subsurface Laser Scattering) for industrial food inspection. To obtain high and uniform quality, in for example dairy products like yoghurt and cheese, it is important to monitor the change in size and shape of microscopic particles over time. In this paper we demonstrate the usefulness of our SLS system for characterizing food items. We use a laser source that can be tuned to any wavelength in the range of 455 nm - 1020 nm by applying an AOTF (Acousto-Optical Tunable Filter) to an optical beam generated by a SuperK (supercontinuum) laser system. In our experiments we show how the system can be used for discriminating dairy products with different structure and how the structural change of a foam can be monitored over time. Time stability of the system is essential for measurements over several hours, and we demonstrate the time stability by measuring the reflectance profile of an inorganic phantom. The SLS technique is a very promising technique for non-intrusive food inspection, especially for homogenous products where particle size and shape are important parameters.

1 Introduction

The purpose of this paper is to present results of our computer vision system for characterizing structural elements in food products. The development of microstructures is important in the production of for example fermented dairy products. Controlling this development, which can take hours or days, is essential for obtaining high quality products while minimizing energy consumption and waist. Our system is based on a supercontinuum (SuperK[1]) laser source that uses an AOTF (Acusto-Optic Tunable Filter) to produce a beam with a precise wavelength that can be tuned over a broad range. The laser system delivers the light through a photonic crystal fiber that is integrated with a camera as illustrated in Figure 1. Based on this system we are able to perform hyperspectral SLS (Sub-surface Laser Scattering) measurements of various food samples. Our SLS system has high potential for becoming an integral part of product development and production, because it provides non-intrusive and objective assessment

[1] http://www.nktphotonics.com/

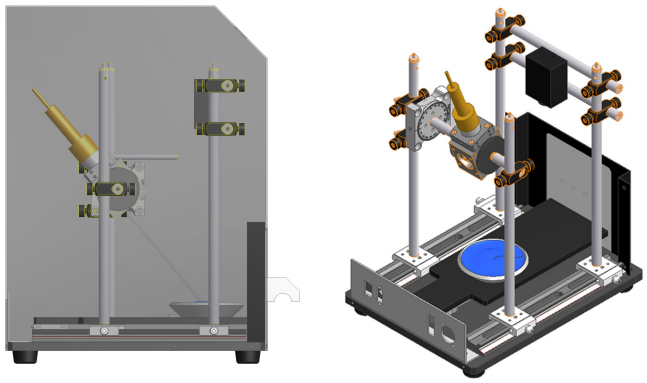

(a) Side view of the hyperspectral SLS vision system.

(b) 3D illustration of the hyperspectral SLS vision system.

Fig. 1. Illustration of the vision systems. In (a) the system is shown from the side where the laser source is at the left side pointing at the sample. The instrument mounted on the right side is the camera. The gray shade behind is the cover, which protects the setup from surrounding light. In (b) the same setup is illustrated from an angle without the cover. Both the laser source and the camera is mounted in a flexible setup that can be adjusted to various positions and angles.

of structure of the food item. Food structure can be coupled to parameters like mouth feel and creaminess [1].

Many food items are processed to change their structure. Protein structure of milk changes by fermentation from being dissociated to form chains. In a whipping process air bobbles are added to the food. Methods like rheology, microscopy and spectroscopy are traditionally used for measuring such changes [3]. The advantage of a vision systems, like our SLS system, is the avoidance of contact with the food and the possibility of implementing an inline application [7]. We will demonstrate how this variation in structural composition can be assessed using our SLS system.

2 Method

We have presented the setup for hyperspectral SLS in [6], and we are continuously developing the system for food inspection problems. The setup is shown in Figure 1, and from the results presented in [6] we have extended the procedure to include improved image acquisition using high dynamic range imaging (HDR). We also demonstrate the time stability of the system and how a process can be monitored over time.

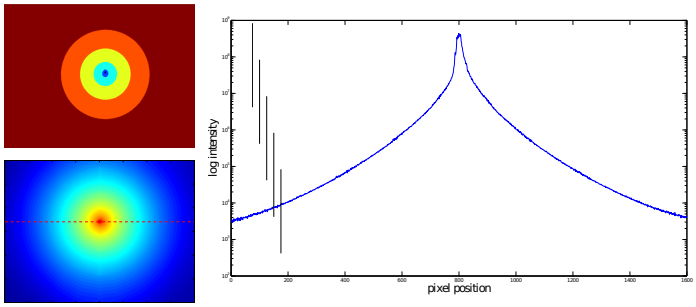

Fig. 2. Building a HDR image. Top left shows a mask used for building the HDR image. The mask with the dark blue color in the center is used as a mask for the image with the shortest exposure time, and the other masks are used with longer and longer exposure times. For each mask the pixel value of the image is divided by the corresponding exposure time. Bottom left shows the HDR image on a log scale, with the highest intensity in the center red part and lowest in the blue parts. Right is a graph of the profile along the dotted line. The vertical lines show the dynamic range of the five differently exposed images for building this HDR image.

2.1 High dynamic range imaging

The subsurface scattering profiles are highly divergent and cannot be covered by the effective dynamic range of the camera. Acquiring images at a number of exposures can solve this, but this will result in large amounts of data to be stored. To overcome this we construct a HDR image. For now we have chosen a simple approach for constructing HDR images by acquiring images with different shutter time and using the shutter time as a multiplicative factor. This approach is illustrated in Figure 2.

An image can contain pixels that are under exposed, well exposed or over exposed or a combination of these. The problem is to combine the well-exposed pixels over all images. We make the simplifying assumption that the image intensity scales linearly with exposure time, which can be expressed as $\mathbf{I}(t) = t\mathbf{I}_n$, where $\mathbf{I}$ is the image, t is the exposure time, n is the number of images and $\mathbf{I}_n$ is the image acquired with the shortest exposure time.

The HDR image is constructed by choosing the pixels from the image with highest signal to noise ratio. The image acquisition results in a stack of images, where the intensity of the pixels increases with increasing exposure time. Assuming the pixel noise to be independent of the exposure time, we will have highest signal to noise ratio for a pixel in the image with the longest exposure time, where that pixel is still not saturated. Therefore, we construct our HDR image by starting with the image acquired with the longest exposure time and choosing all non-saturated pixels. After that we choose the image with the second longest exposure time, and add all the unsaturated pixels that was not chosen until now, multiplied with a factor $\tau_i = \frac{t_1}{t_i}$, where $i = 2$ for the second image. We continue

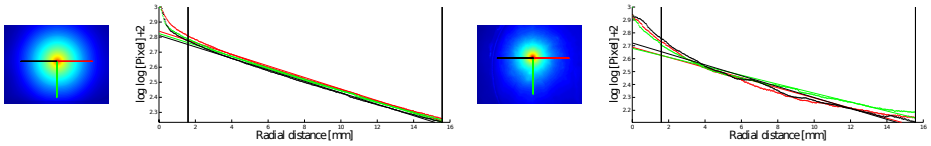

Fig. 3. Characterization of two samples – (*left*) a phantom and (*right*) a whipped cream foam. The HDR image shows the three profiles marked with a black (*backward scattering*), a red (*forward scattering*) and a green line(*orthogonal profile*). The sample is illuminated from the left. The iterated logarithm of the intensity is shown in the three curves colored similar to the profiles in the image, and the straight lines are the fitted curves. The model is only partly applicable and the vertical line shows the minimum radial distance for the fit.

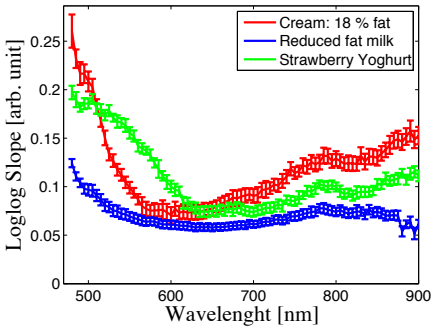

Fig. 4. Iterated logarithmic characterization as a function of wavelength for various products. The primary difference between cream and milk is the content of fat globules, and the primary difference between milk and yoghurt is the fermentation where protein structures change due to acidification. Both these differences are clearly distinguishable from the SLS characterization. The error bars are error on the slope estimate of the iterated logarithm.

this way until all images are added. If the image with the shortest exposure time contains saturated pixels, these are added to the final HDR image.

2.2 Sample characterization

The iterated logarithm of the intensity ($\log(\log(\mathbf{I}))$) presented in [2] and [6] was used for analyzing the scattering distribution. We have extended the number of profiles through the image since an oblique incident of 45° illumination was used. The oblique illumination results in a anisotropic shape of the intensity peak. Mie-theory predicts a symmetric scattering profile orthogonal to the direction of the incoming light, which has been verified in [5]. Based on this we have extended the characterization using three profiles all starting from the intensity peak – two in the incident direction of the beam and one perpendicular to this. This way we capture some of the anisotropy in the scattering distribution. This is

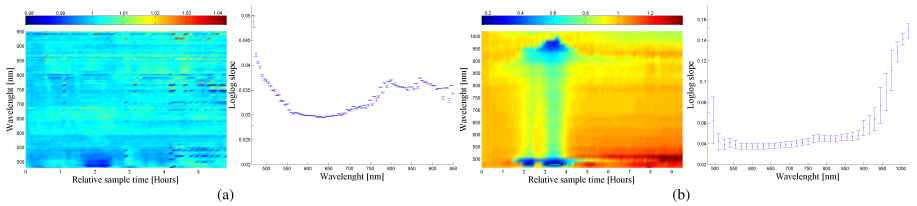

Fig. 5. Development of the SLS characterization over time. (a) time development of a phantom object and (b) time development of whipped cream. Left the SLS characterization (normalized) is shown as an image and right the average SLS parameter with error bars of one standard deviation. The phantom has almost no change over time, showing that the system is very stable, whereas the whipped cream changes significantly.

illustrated in Figure 3. But the resulting characterization based on the slope and offset of the fitted curve was very similar, so in the rest of this paper we just use the average of the three profiles.

3 Experiment and results

We have performed experiments to demonstrate how the system can be used for assessing changes over time. In Figure 4 this is shown for some commercially available dairy products, which shows that for most wavelengths there is a clear difference in their characterization. The fermentation of milk to form yoghurt changes the shape of the SLS parameter significantly.

3.1 Monitoring the time development of the scattering profile

To estimate the system stability we have measured the SLS profile of a phantom. The phantom is solid block containing polystyrene spheres made similar to the description in [4]. We measured the phantom over 5 hours and 50 minutes with wavelengths ranging from 460 nm to 1020 nm. In a similar way we measured the development of whipped cream, which is foam that changes structure over time. Scattering parameters of both phantom and whipped cream are presented in Figure 5. The measurements of the phantom are stable over time with minor variations due to noise in the measurements, whereas the whipped cream clearly changes with time as the foam collapses.

4 Discussion and conclusion

The main contributions of this paper is the demonstration of the SLS system for time studies and a HDR imaging for improved SLS characterization. The anisotropic shape of the scattering center is also characteristic for the food items. Our characterization, based on the linear fit of the iterated logarithm,

did not show the expected directional dependence, but using the anisotropy is very promising for future research.

The HDR imaging improves characterization, because the entire dynamic range is captured making it possible to measure the entire reflectance profile. This allows the SLS parameters to be estimated from a larger number of pixels and a much higher dynamic range, than using just one exposure. In addition we obtain a good characterization also in regions where the camera sensitivity or beam power is very low or very high. Images based on a single exposure would have a risk of being under or over exposed. Our procedure for building the HDR images also ensures a selection of the pixels with highest signal to noise ratio while being simple and fast.

Our SLS system is highly flexible because it offers a high spectral resolution and a high variation in geometric configuration. This makes it a unique instrument for SLS characteristics of food items, and our research will focus on finding combined radiometric and geometric configurations that optimally characterizes the food sample. From this we will be able to design a new type of vision systems for improved food quality assessment.

5 Acknowledgements

This project was carried out in the Center for Imaging Food Quality supported by The Danish Council for Strategic Research[2].

References

1. M.C. Bourne. *Food texture and viscosity: concept and measurement*. Academic Pr, 2002.
2. J. M. Carstensen and F. Møller. Online monitoring of food processes using subsurface laser scattering. In *Advances in process analytics and control technologies (APACT 09), 2009, Glasgow, Scotland, May 5-7*, 2009.
3. P. Fischer and E. J. Windhab. Rheology of food materials. *Current Opinion in Colloid & Interface Science*, 2010.
4. G. Marquez and LH Wang. White light oblique incidence reflectometer for measuring absorption and reduced scattering spectra of tissue-like turbid media. *Opt. Express*, 1(13):454–460, 1997.
5. S. Menon, Q. Su, and R. Grobe. Determination of g and μ using multiply scattered light in turbid media. *Physical review letters*, 94(15):153904, 2005.
6. O. H. A. Nielsen, A. L. Dahl, R. Larsen, F. Møller, F. Donbæk, C. L. Thomsen, H. Aanæs, and J. M. Carstensen. Supercontinuum light sources for hyperspectral subsurface laser scattering - applications for food inspection. In 2011 Proceedings SCIA, editor, *Scandinavian Conference on Image Analysis, Ystad, Sweden, May 2011*, Lecture Notes in Computer Science. Springer, may 2011.
7. D. W. Sun. *Hyperspectral imaging for food quality analysis and control*. Academic Press, 2010.

[2] http://www.cifq.dk